Journal of Atmospheric and Solar-Terrestrial Physics 136 (2015) 187–200

Contents lists available at ScienceDirect

Journal of Atmospheric and Solar-Terrestrial Physics

journal homepage: www.elsevier.com/locate/jastp

Interannual and intraseasonal variability of stratospheric dynamics and stratosphere–troposphere coupling during northern winter

A.I. Pogoreltsev [a,*], E.N. Savenkova [b], O.G. Aniskina [a], T.S. Ermakova [a], W. Chen [c], K. Wei [c]

[a] Russian State Hydrometeorological University, Maloohtinsky 98, St. Petersburg 195196, Russia
[b] St. Petersburg State University, ul. Ulyanovskaya 1, St. Petersburg 198504, Russia
[c] Center for Monsoon System Research, Institute of Atmospheric Physics, Chinese Academy of Sciences, Beijing 100080, China

ARTICLE INFO

Article history:
Received 20 April 2015
Received in revised form
11 August 2015
Accepted 19 August 2015
Available online 10 September 2015

Keywords:
Interannual and intraseasonal variability
Sudden stratospheric warming
Planetary waves
Wave activity flux

ABSTRACT

The UK Met Office reanalysis data have been used to investigate the interannual and intraseasonal variability of the stratospheric dynamics and thermal structure. The results obtained show that the maximum of interannual variability of the mean zonal flow associated with the quasi-biennial oscillation (QBO) is observed at the altitude of about 30 km. It is shown that there is a statistically significant influence of the QBO phase on the extratropical stratosphere, the so-called, Holton–Tan effect. The results of data analysis show that the conditions under the easterly QBO phase are more favorable for the development of the sudden stratospheric warmings (SSW). The statistical analysis of 15 major SSW observed during two last decades has been performed. The obtained results demonstrate that in recent years internal processes associated with nonlinear interactions of stationary planetary waves (SPW) with the mean flow played a dominant role. It is shown that the first enhancement of the SPW1 in the upper stratosphere takes place because of an amplification of nonlinear interactions between this wave and the mean flow. This enhancement is accompanied by a subsequent increase in the wave activity flux from the stratosphere into the troposphere with further redistribution of wave activity in the horizontal plane. Then, an increase of the upward flux from the troposphere into the stratosphere in another region occurs. The secondary enhancement of the planetary wave activity in the stratosphere is accompanied by the heating of the polar region and the weakening, or even reversal of the stratospheric jet. Additionally to the well-known result that meridional refraction of SPW to the polar region in stratosphere is one of the preconditions of development SSW, the nonlinear wave–wave and wave–mean flow interactions can play an important role before and during SSW. It is shown that the upper stratosphere can be considered as the region where SPW2 is generated during SSW.

1. Introduction

Sudden stratospheric warming (SSW) events are prominent processes, during which the troposphere and stratosphere demonstrate the dynamical coupling (Holton, 1980; McIntyre, 1982). According to the existing notions (Stan and Straus, 2009), SSW events may develop due to two reasons: an increase of wave activity flux from the troposphere into the stratosphere (the so-called classic scenario suggested by Matsuno, 1971), and/or caused by the internal dynamical processes, that, as the result of nonlinear interactions of planetary waves with the mean flow at the stratospheric heights (Scott and Polvani, 2006; Pogoreltsev, 2007). Unfortunately, these two mechanisms compliment each other and it is difficult to estimate their relative contribution. The interest in studying SSW events increased substantially in recent years. This increase is primarily due to the obtained results that indicate a significant influence of the SSW on the formation of the weather anomalies in the troposphere (Baldwin and Dunkerton, 2001; Baldwin et al., 2007; Sun and Robinson, 2009; Waugh et al., 2010). It has been found that the SSW events affect the dynamics and energetics of the upper atmosphere (the mesosphere and even the thermosphere) (Siskind et al., 2010; Kurihara et al., 2010; Fuller-Rowell et al., 2010; Funke et al., 2010; Liu et al., 2011; Yuan et al., 2012), that is, they can influence the coupling to space weather, and manifest in the characteristics of ionospheric disturbances (Pedatella and Forbes, 2010; Pancheva and Mukhtarov, 2011). During the last decades, the growth of amplitude of stationary planetary wave with zonal wave number one (SPW1) has been observed in the stratosphere and, as a consequence, the nonlinear interaction of this wave with the mean flow becomes stronger (Pogoreltsev et al., 2009). This leads to rising intensity of irregular fluctuations, the so-called stratospheric vacillations (Holton and

* Corresponding author. Fax: +7 812 4446090. Tel.:+78126330174
E-mail address: apogor@rshu.ru (A.I. Pogoreltsev).

http://dx.doi.org/10.1016/j.jastp.2015.08.008
1364-6826/

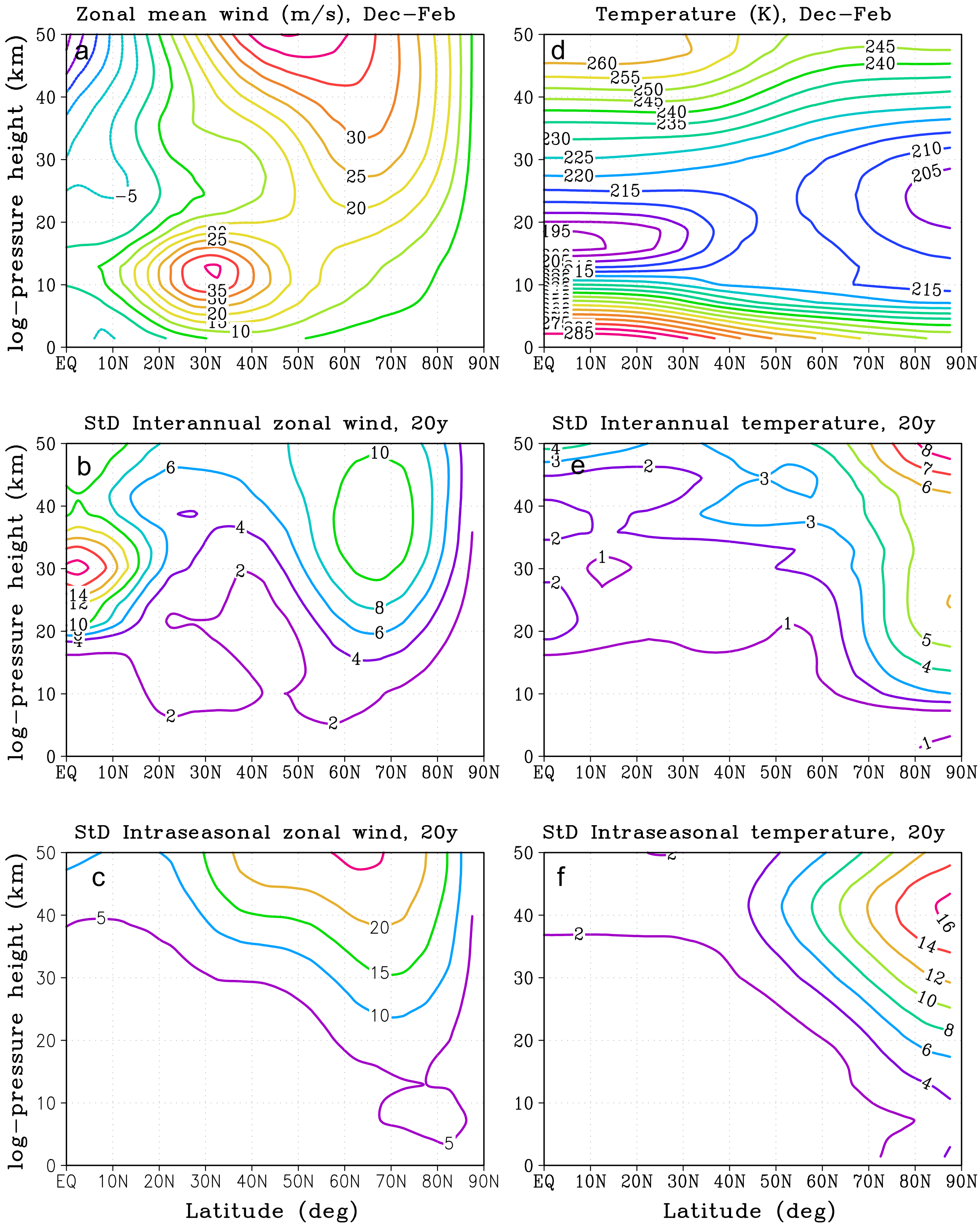

Fig. 1. Left panels show the characteristics of the zonal mean flow: climatic distribution (a), standard deviations of the interannual variability (b), and standard deviations of the intraseasonal variability (c). Right panels show the same for temperature: climatic distribution (d), standard deviations of the interannual variability (e), and standard deviations of the intraseasonal variability (f).

Mass, 1976).

Despite the growing interest in the study of the SSW and its impact on the weather, climate, and upper atmosphere, including the ionosphere, the most of papers only present results of analysis of the SSW distinctive features observed over recent years (Labitzke and Kunze, 2009; Ayarzaguena et al., 2011; Kuttippurath and Nikulin, 2012). The problem of possible mechanisms responsible for SSW forcing is widely discussed in recent publications. For instance, see Esler et al. (2006), Albers and Birner (2014), and reference therein. Nevertheless, the questions concerning the source and/or the cause of the arising SSW are still open (Sun et al., 2011). Analysis of the dynamic processes in the stratosphere based on the UK Met Office data (for the description see Swinbank and O'Neill, 1994) has demonstrated that, during the recent decades (1992–2012), a reassessment of the relative role of different mechanisms responsible for initiating SSW events has occurred. In recent years, internal processes associated with nonlinear interactions of planetary waves with the mean flow played a predominant role. A lack of attention to the internal dynamic processes in the analyses of SSW events has also been noted in the recent paper by Labitzke and Kunze (2009). To investigate the preconditions, origin, and development of the SSW events, both the dynamical coupling with the troposphere and the nonlinear wave–mean flow and wave–wave interactions in the upper stratosphere have to be considered. The main objectives of the present study are the following: to investigate the interannual and intraseasonal variability of the zonal mean flow and temperature in the stratosphere; to consider the wave–wave and wave–mean flow nonlinear interactions before and during SSW; and to explain the physical mechanisms that are responsible for the development of SSW events and associated wind reversals occurring in the Northern winter.

2. Data and methods

To investigate the climatological features and variability of the stratospheric dynamics, the UK Met Office assimilated fields (Swinbank and O'Neill, 1994) have been used. These data are available for the last several decades, which is a long enough period to reveal most of the climatological features and variability of planetary waves in the stratosphere (Scaife et al., 2000). These meteorological fields were presented at each latitude and altitude in the form of Fourier-series expansions with the set of zonal harmonics with wave numbers $m=0$–4, that is, as a sum of zonally averaged values and the largest planetary waves. The analysis of UK Met Office data shows that, during the last decades, SSW events are mainly observed in the upper stratosphere (between 40 and 60 km). Therefore, it is convenient to reconsider the adopted classification based on the behavior of the zonal flow and/or temperature at 10 hPa (altitude of about 30 km) (Labitzke, 1977; Labitzke and Naujokat, 2000; Labitzke et al., 2005; Charlton and Polvani, 2007; Butler et al., 2015). For instance, in January 2012 there was no any reversal of the zonal wind at 30 km, while the strong reversal and temperature increase in the polar region occurred in the upper stratosphere. Thus, the day of zonal mean wind reversal at middle latitude anywhere between 40 and 50 km is used in the present study to determine the central date of the SSW. To investigate the wave–wave and wave–mean flow nonlinear interactions, the terms of eddy potential enstrophy balance equation have been calculated using the composite meteorological fields. The 3D wave activity and Eliassen–Palm fluxes have been considered to estimate the role of stratosphere–troposphere coupling in the development of the SSW events.

3. Variability of the stratospheric dynamics and thermal structure

Before analyzing the SSW events, it is helpful to consider the interannual and intraseasonal variability of the zonal mean flow and temperature observed during the Northern winter seasons (December–February) in the last two decades. Upper panels of Fig. 1 show distributions of the zonal mean flow (a) and temperature (d) in the Northern Hemisphere averaged over 1992–2011. The middle panels of Fig. 1 demonstrate the standard deviations of the interannual variability of annual winter means of these fields. One can see that the main interannual variability of the mean flow is observed above the equator at the altitude of about 30 km (b), and this variability is caused by the well-known quasi-biennial oscillation (QBO) (Baldwin et al., 2001). There exists also a weaker variability of the mean flow at middle latitudes, and the temperature at high latitudes in the stratosphere. The lower panels of Fig. 1 show the standard deviations of the intraseasonal variability of the zonal mean flow (c) and temperature (f) during December–February obtained using daily values and then averaged over 20 years (1992–2011). The maximum of intraseasonal changes of the zonal wind is located at the middle latitudes in the upper stratosphere, and this variability can be linked to nonlinear interactions of the mean flow with planetary waves during the vacillation cycles and/or due to development of the SSW events. The intraseasonal variability of the temperature occurs in the higher latitudes with the maximum observed in the polar region at about 40 km (Fig. 1f). When calculating the intraseasonal variability presented in Fig. 1, the initial time series have been detrended, that is, the climatic seasonal changes of the zonal wind and temperature have been excluded.

For the further analysis the QBO phase was determined according to the deviation of the equatorial zonal mean flow from the climatic-mean values at the altitude of about 30 km (10 hPa pressure level) instead of 40–50 hPa pressure level, as has been made in the paper of Holton and Tan (1980). Positive and negative differences correspond to the westerly and easterly QBO phases (wQBO and eQBO, respectively). Following Pogoreltsev et al. (2014) we calculated the averaged zonal mean distributions of the zonal wind and temperature for the derived westerly (1993, 1995, 1997, 1999, 2002, 2004, 2006, 2008, and 2011) and easterly (1994, 1998, 2000, 2001, 2003, 2005, 2007, 2010, and 2012) QBO phases for December–February. The differences in the zonal mean wind and temperature between the westerly and easterly QBO phases (wQBO–eQBO) are presented in Fig. 2 (upper and lower panels, respectively). The polar stratospheric temperature averaged over years with the easterly QBO phase is higher (the difference in temperature under wQBO and eQBO is negative), and the polar vortex is weaker.

To estimate the statistical significance of the QBO influence on the extratropical stratosphere, the so-called Welch's t-test has been used (Welch, 1947):

$$t = \frac{|\bar{X}_w - \bar{X}_e|}{\sqrt{S_w^2/N_w + S_e^2/N_e}}, \tag{1}$$

where $\bar{X}_w$ and $\bar{X}_e$ are the values averaged over westerly and easterly years of QBO, S_w and S_e are the standard deviations, and N_w and N_e are the sample size in the westerly and easterly years of QBO. The degree of freedom ν associated with this variance is estimated as

$$\nu = \frac{(S_w^2/N_w + S_e^2/N_e)^2}{(S_w^2/N_w)^2/(N_w - 1) + (S_e^2/N_e)^2/(N_e - 1)}. \tag{2}$$

Several recent studies of the QBO influence on the extratropical circulation have performed statistical analysis using this approach (Naoe and Shibata, 2010; Inoue et al., 2011). The results of statistical levels calculations are presented in Fig. 2 by contours. This figure shows that statistical significance of the zonal wind changes in the tropical stratosphere is very high (more then 99%). The statistical significance of the zonal wind changes in the extratropical stratosphere is lower, nevertheless, it is of about 95%. The statistical significance of the temperature changes in the polar upper stratosphere depending on QBO phase is more than 90%. The results obtained allow us to assume that, on the average, SSW events during the easterly QBO phase are more intensive, and/or the frequency of these events is higher.

4. Statistical analysis of the SSW

To understand the preconditions and evolution of the SSW, a statistical model of these events has been developed based on the UK Met Office data. Fifteen major SSW events that were observed

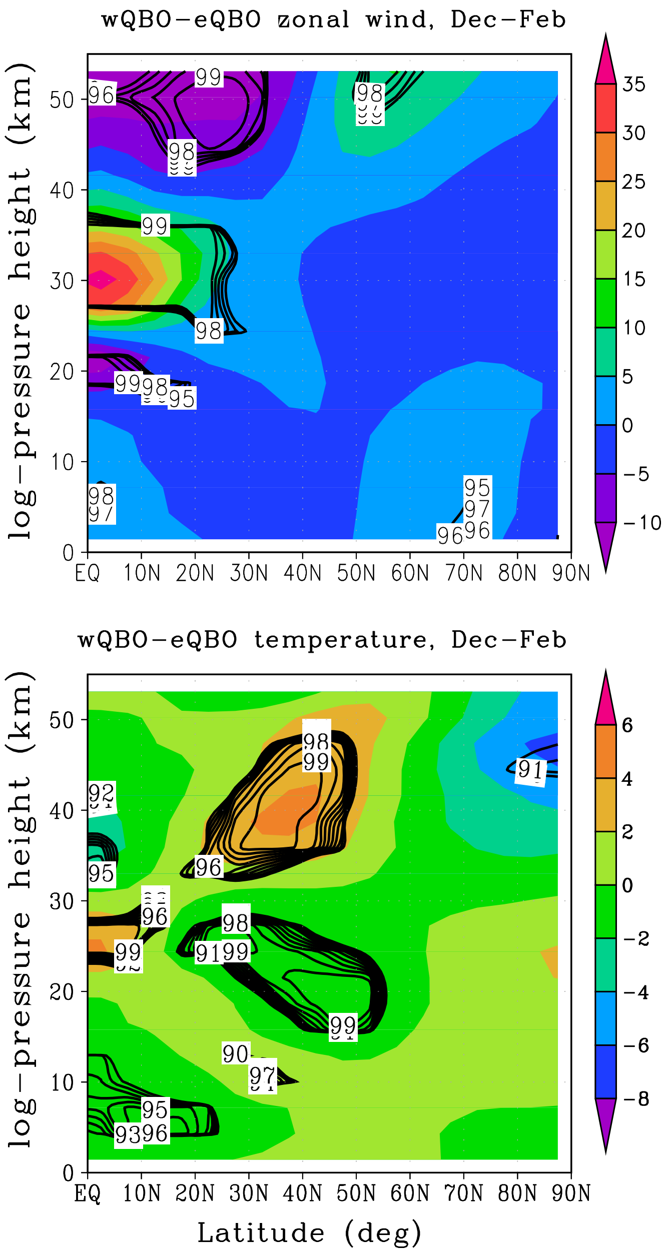

Fig. 2. Composite differences in zonal mean wind (upper panel) and temperature (lower panel) between westerly and easterly QBO phases (wQBO–eQBO). Lines show the significance levels above 95% for wind and above 90% for temperature.

Table 1
Dates of the major SSW events observed in January–February 1992–2012.

Year	Dates of the SSW	QBO phase
1992	January 13	we-QBO
1993	February 22	w-QBO
1995	January 30	w-QBO
1996	February 18	we-QBO
1998	February 7	e-QBO
1999	February 26	w-QBO
2000	February 7	e-QBO
2001	January 29	e-QBO
2002	February 17	w-QBO
2003	January 15	e-QBO
2008	February 7	w-QBO
2009	January 23	ew-QBO
2010	January 30	e-QBO
2011	January 31	w-QBO
2012	January 18	e-QBO

in January–February of 1992–2012 years have been selected (Table 1). There are years when the QBO-phase change happens. Reversal of the zonal wind from westerly to easterly or vice versa occurs in the lower and middle stratosphere. These years are indicated as we-QBO and ew-QBO in Table 1.

To build the statistical model, the composite of meteorological fields (zonal and meridional components of the wind, temperature and geopotential height) for these 15 events have been constructed.

It should be noted that our definition of the SSW central date differs from that suggested by the WMO, who defined it as the first day of zonal wind reversal at 10 hPa pressure level and 60°N (Charlton and Polvani, 2007; Butler et al., 2015). Although sometimes our definition coincides with the conventional one (for instance, in February 1999 and 2002), the central date of the SSW in January–February 2001 substantially differs from that in Charlton and Polvani (2007). To understand this difference, consider the behavior of the zonal mean wind and temperature during the 2000–2001 winter. The time–altitude cross-sections of the amplitude of zonal harmonics with $m=1$ in the geopotential height and mean zonal wind at 62.5°N as well as the changes of zonal mean temperature at 87.5°N from December to March are presented in Fig. 3. Indeed, the reversal of the zonal wind at 30 km is observed on 11 February as noted in Charlton and Polvani (2007) (see Table 1 in this paper). Nevertheless, if one considers the

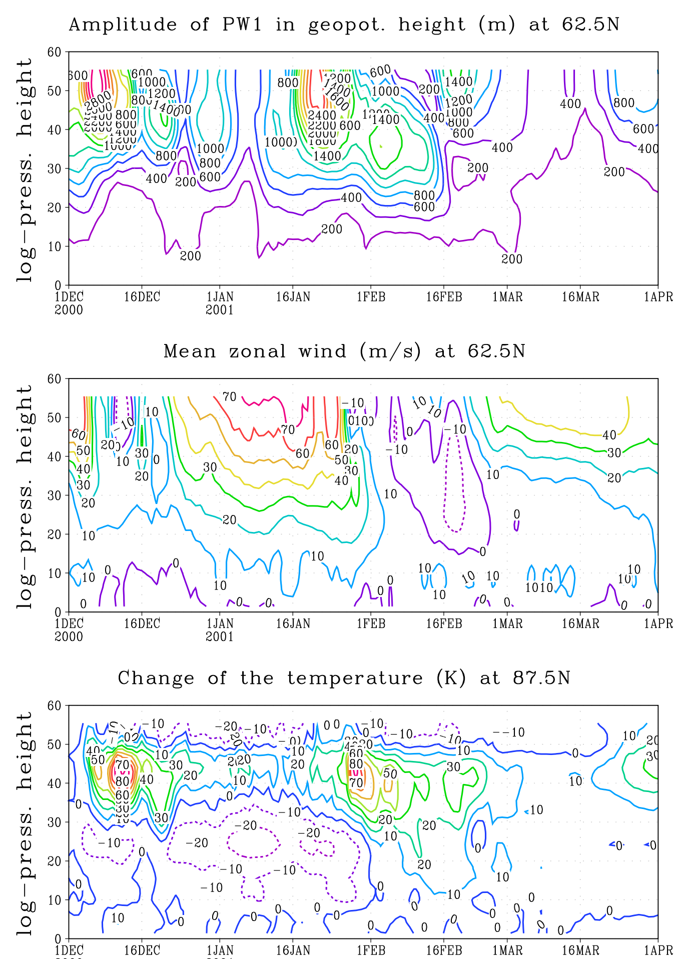

Fig. 3. The time–altitude cross-sections of the amplitude of the zonal harmonic with $m=1$ in the geopotential height and the mean zonal wind at latitude 62.5°N (upper and middle panels, respectively) observed in 2000–2001 winter. The changes of the zonal mean temperature during December–March at latitude 87.5°N are shown in the lower panel.

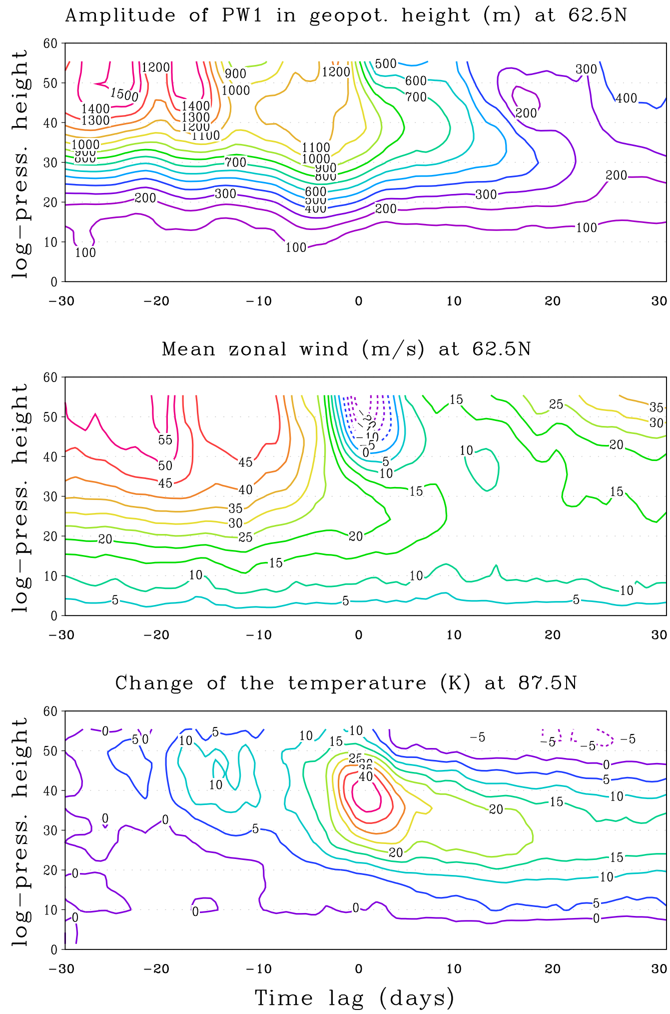

Fig. 4. Log-pressure height–time-lagged composite plots of the UK Met Office meteorological fields: the amplitude of zonal harmonic with $m=1$ in the geopotential height and the mean zonal wind at latitude 62.5°N (upper and middle panels, respectively). Lower panel shows the changes of the mean temperature during 30 days before and 30 days after the SSW event at latitude 87.5°N.

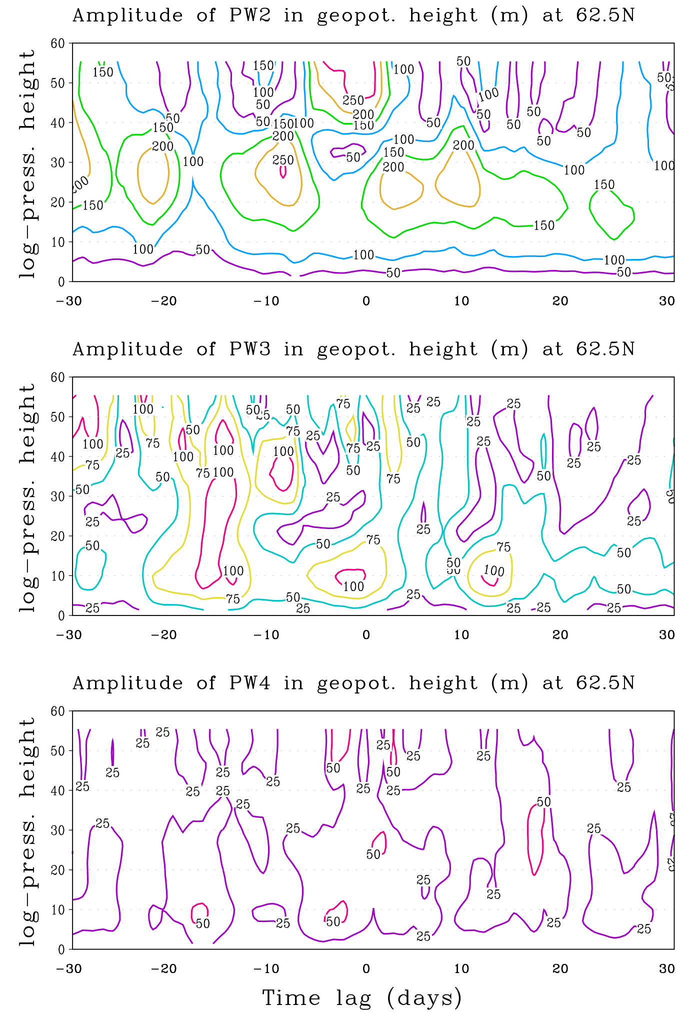

Fig. 5. Log-pressure height–time-lagged composite plots of the UK Met Office meteorological fields: the amplitudes of zonal harmonics with $m=2$–4 in the geopotential height at latitude 62.5°N (upper panel for wave number 2, middle for wave number 3, lower for wave number 4).

behavior of the zonal wind and temperature in the upper stratosphere, one can notice that the reversal of the zonal wind and warming of polar region took place substantially earlier (by about two weeks), and at 30 km we observe only the effects of downward propagation of this event. Thus, we conclude that the formal definition of the SSW central date based on the wind reversal and/or temperature changes at 30 km is not always acceptable, and one has to consider the behavior of these fields at higher altitudes. The results on the intraseasonal variability of the zonal mean wind and temperature presented in Fig. 1 (panels c and d) allow us to suggest that the zonal wind has to be analyzed at the middle latitudes in the upper stratosphere, and temperature changes have to be considered at the altitude of about 40 km (instead of 30 km) in the polar region, as has been done in Table 1.

The composite distributions of meteorological fields for 61 days (30 days before and after the event) have been calculated by averaging over all chosen SSWs. The distributions have been separated into the zonal mean components and zonal harmonics with $m=1$–4. These results are presented in Figs. 4 and 5. Fig. 4 shows an enhancement of the SPW1 about 20 days before the SSW event, which is not accompanied by a warming of the polar stratosphere and noticeable weakening of the zonal mean flow. The second enhancement of the zonal harmonic with $m=1$ occurs just before the SSW event, and is accompanied by the reversal of the zonal wind direction and a strong increase of temperature (up to 60 K) in the polar region at about 40 km. During the SSW event, an increase of the amplitudes of zonal harmonics with $m=2$ is also observed in the upper stratosphere (Fig. 5). It, however, does not extend down to the troposphere.

5. Wave–wave and wave–mean flow nonlinear interactions

To consider the effects of nonlinear interactions, the terms contributing to the balance of eddy enstrophy have been calculated. The general form of the eddy enstrophy balance equation is the following (Smith, 1983):

$$\frac{\partial}{\partial t}\frac{\overline{q'^2}}{2} + \overline{\frac{q'u'}{a\cos\varphi}\frac{\partial q'}{\partial\lambda}} + \overline{\frac{q'v'}{a}\frac{\partial q'}{\partial\varphi}} + \frac{\overline{q'v'}}{a}\frac{\partial\bar{q}}{\partial\varphi} = \overline{q'Q'}, \tag{3}$$

where q' is the perturbation of the quasi-geostrophic potential vorticity, u' and v' are perturbations of the zonal and meridional geostrophic winds, and Q' represents the perturbation of diabatic sources and sinks and terms describing the subscale contributions to the momentum equation. All other symbols have their conventional meaning. The first term in left-hand side denotes the wave transience. The two next terms describe the wave–wave interactions. The last term in the left-hand side describes the eddy enstrophy changes due to wave–mean flow interactions. The term in the right-hand side gives the changes in eddy enstrophy due to the diabatic heating and subscale contributions to the momentum equation including momentum deposition by gravity and inertial-gravity waves).

To calculate the contribution of different terms to the eddy enstrophy balance for wave 1, we use slightly different expressions than was suggested by Smith (1983, Appendix). The second line in the terms describing the interactions wave1 and wave2 may be written as follows:

$$+\frac{1}{4a\cos\varphi}[2U_2Q_1^2Q_1^{*2} + U_2^*(Q_1^{*2} - Q_1^2)]$$

$$+\frac{1}{4a}\left[(V_2Q_1 + V_2^*Q_1^*)\frac{\partial}{\partial\varphi}Q_1 + (V_2^*Q_1 - V_2Q_{1*})\frac{\partial}{\partial\varphi}Q_1^*\right]. \tag{4}$$

The notations are the same as in Smith (1983). This term can be rewritten in a different way using the quasi-geostrophic eddy continuity equation for wave2 as was suggested in Smith et al. (1984):

$$+\frac{1}{8a\cos\varphi}\frac{\partial}{\partial\varphi}\{[V_2(Q_1^2 - Q_1^{*2}) + 2V_2^*(Q_1Q_1^*)]\cos\varphi\}. \tag{5}$$

The comparison of the results obtained using Eqs. (4) and (5)

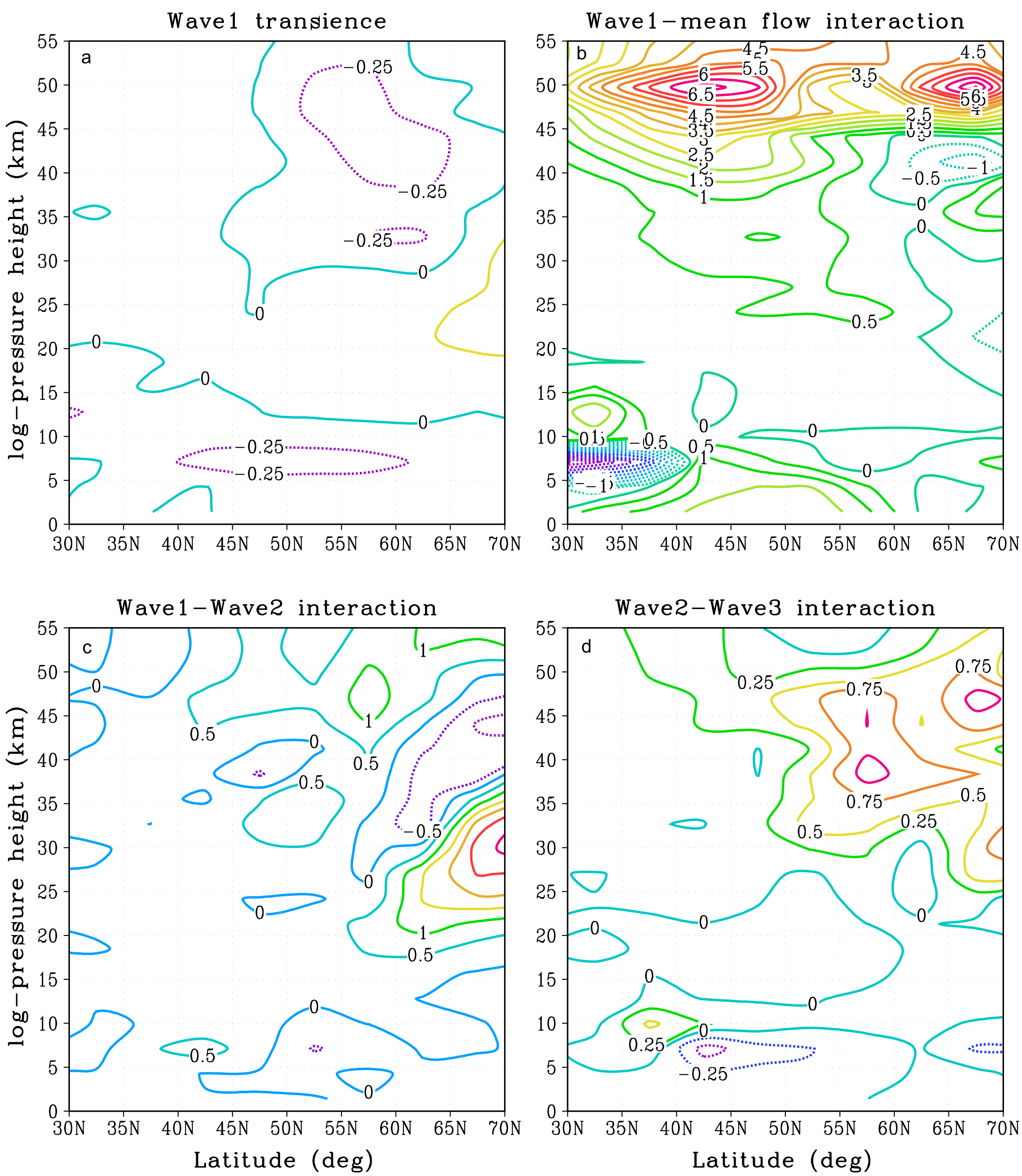

Fig. 6. Latitude–height cross sections of terms contributing to the enstrophy balance for wave1 averaged over 10 days before SSW: transience (a), wave–mean flow interaction (b), wave1–wave2 (c) and wave2–wave3 (d) interactions. Units are 10^{-15} s^{-3}.

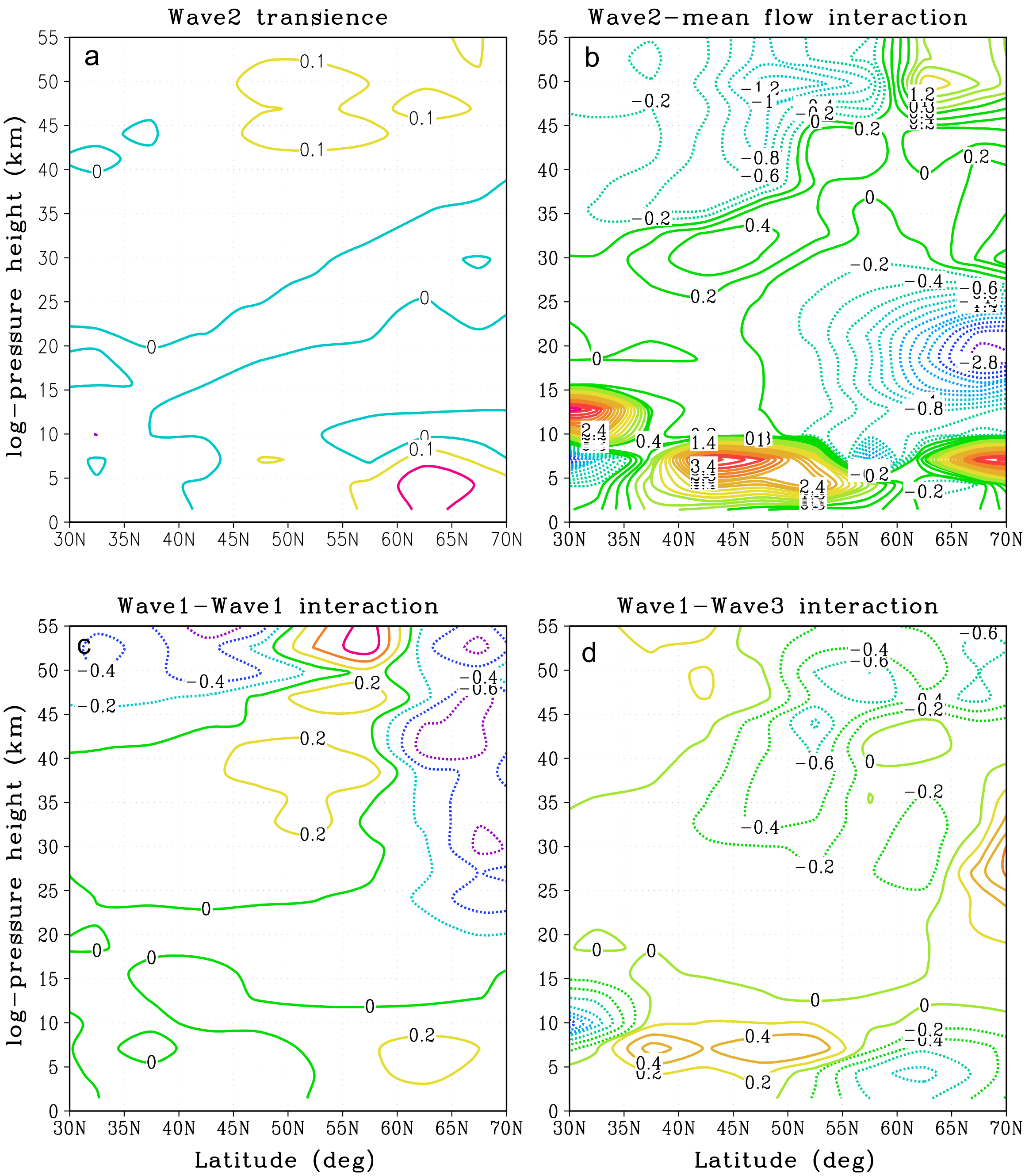

Fig. 7. Latitude–height cross sections of terms contributing to the enstrophy balance for wave2 averaged over 10 days before SSW: transience (a), wave–mean flow interaction (b), wave1–wave1 (c) and wave1–wave3 (d) interactions. Units are 10^{-15} s^{-3}.

shows that there are substantial differences at least in the middle latitude winter stratosphere where the nonlinear wave–wave interactions are strong. It should be noted also that there are misprints in the first line of terms describing interactions of wave1 with waves2 and wave3 (see Smith, 1983, Appendix). The correct line has to be written as follows:

$$+\frac{3}{4a\cos\varphi}[U_2(Q_1Q_3^* - Q_1^*Q_3) - U_2^*(Q_1^*Q_3^* - Q_1Q_3)]. \qquad (6)$$

Latitude–height cross sections of terms contributing to the enstrophy balance for the wave1 and wave2 averaged over 10 days before SSW are shown in Figs. 6 and 7. These figures show that nonlinear wave–wave interactions are stronger at the higher-middle latitudes in the stratosphere. Wave1–mean flow interaction has two maxima in the upper stratosphere at the lower-middle and higher-middle latitudes. Wave2–mean flow interaction is stronger in the troposphere and in the lower stratosphere at high latitudes. The terms contributing to the enstrophy balance for wave1 (a) and wave2 (b) at 30 and 50 km, the transience (black lines), wave1–wave2 and wave1–wave1 interactions (blue lines), wave2–wave3 and wave1–wave3 interactions (green lines), and wave–mean flow interactions (red lines) are presented in Figs. 8 and 9, respectively. The values have been averaged over the middle latitude region from 57.5 to 72.5°N, using cosine of latitude weighting. These figures show that there are the nonlinear interactions between waves before the SSW, while during the SSW event, the wave–mean flow interactions increases, and the eddy potential enstrophy of planetary waves decreases. It should be noted that before the SSW wave-2 transience term (black line) is approximately out of phase with the sum of wave–wave

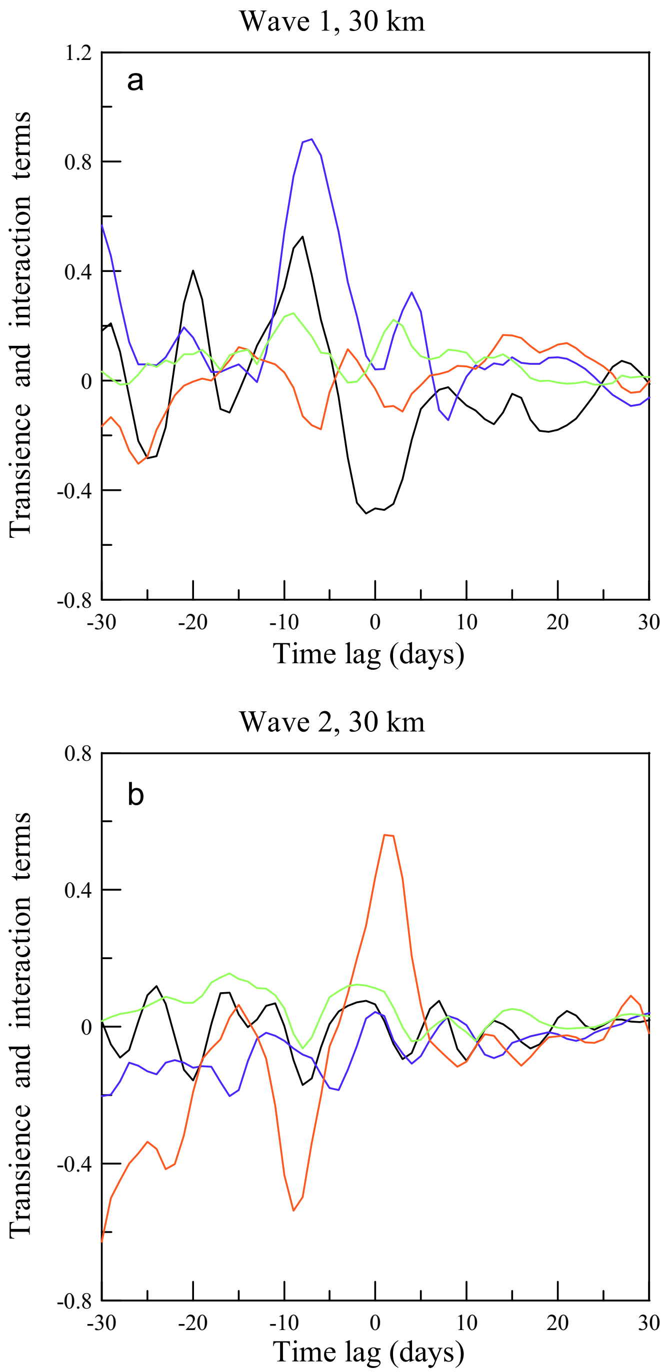

Fig. 8. Terms contributing to the enstrophy balance for wave 1 (a) and wave 2 (b) at 30 km: transience (black lines), wave1–wave2 and wave1–wave1 interactions (blue lines), wave2–wave3 and wave1–wave3 interactions (green lines), and wave–mean flow interactions (red lines). The values have been averaged over a midlatitude region from 57.5 to 72.5°N, using cosine of latitude weighting. Units are 10^{-15} s^{-3}. (For interpretation of the references to color in this figure caption, the reader is referred to the web version of this paper.)

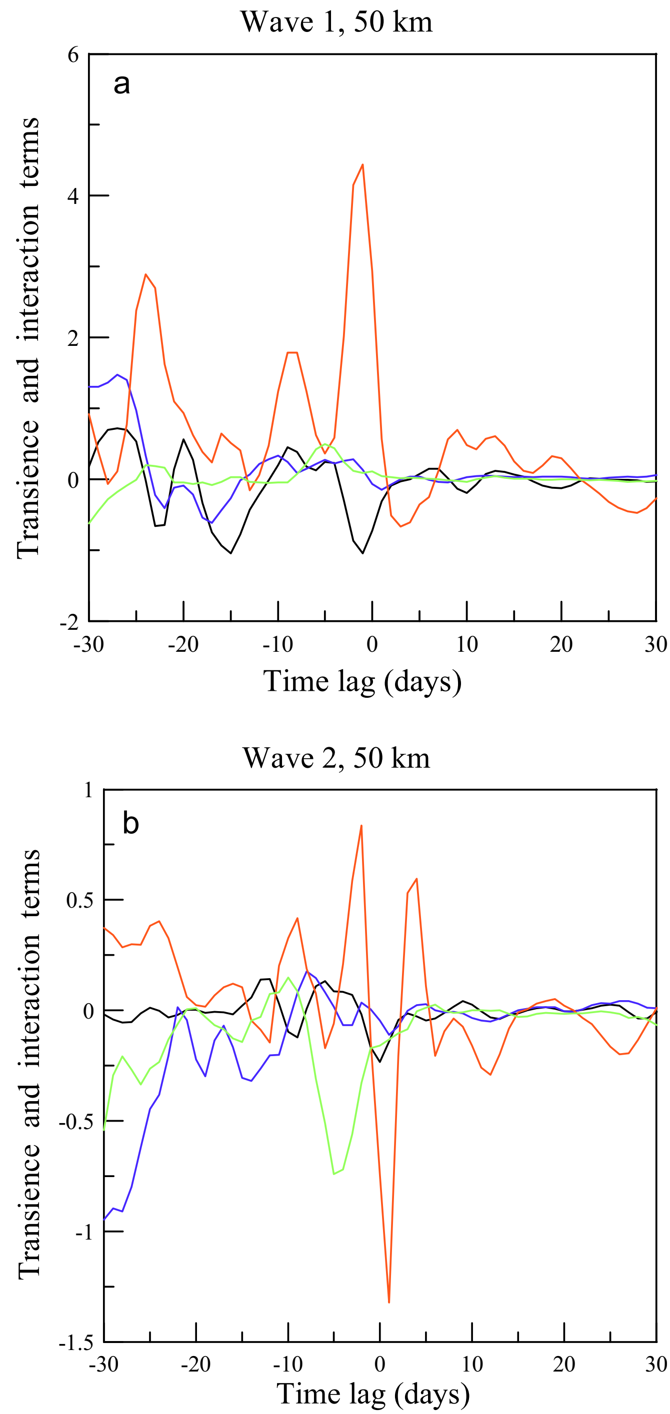

Fig. 9. Terms contributing to the enstrophy balance for wave 1 (a) and wave 2 (b) at 50 km: transience (black lines), wave1–wave2 and wave1–wave1 interactions (blue lines), wave2–wave3 and wave1–wave3 interactions (green lines), and wave–mean flow interactions (red lines). The values have been averaged over a midlatitude region from 57.5 to 72.5°N, using cosine of latitude weighting. Units are 10^{-15} s^{-3}. (For interpretation of the references to color in this figure caption, the reader is referred to the web version of this paper.)

interaction terms (blue and green lines). This result illustrates that the variability of wave-2 activity in the stratosphere is caused mainly by the processes of nonlinear wave–wave interactions. During the SSW event and in the upper stratosphere (Fig. 9) the wave–mean flow interaction dominates.

6. Stratosphere–troposphere coupling

Three-dimensional wave activity flux and its divergence have been calculated to estimate the dynamical coupling between the stratosphere and troposphere during the initiation and development of the SSW event. Three-dimensional flux of wave activity **F** describes the propagation of planetary wave packets (without separation into zonal harmonics) in the longitude (Fx), latitude (Fy), and vertical (Fz) directions. The components of this flux can be expressed as follows (Plumb, 1985):

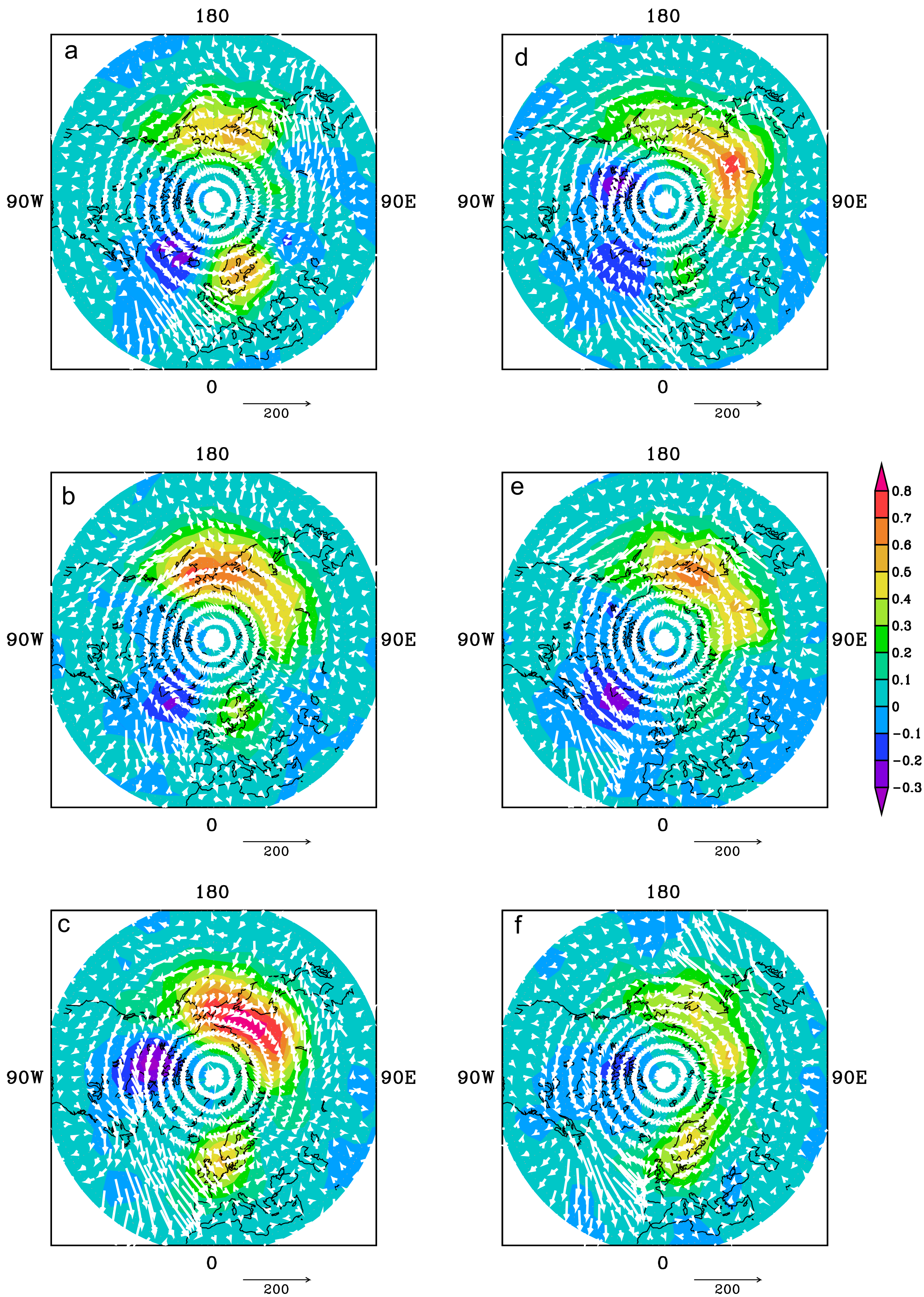

Fig. 10. Longitude–latitude distributions of the vertical component of the wave activity flux at 20 km (shaded) and the horizontal vector at 4 km of the wave activity flux (arrows) at 15 and 10 days before the SSW event (a and b), during SSW (c), and at 5, 10, and 15 days after the SSW event (d, e, and f, respectively).

$$\mathbf{F} = \frac{p}{p_0}\cos\varphi \begin{pmatrix} v'^2 - \dfrac{1}{2\Omega a \sin 2\varphi}\dfrac{\partial(v'\phi')}{\partial\lambda} \\ -u'v' + \dfrac{1}{2\Omega a \sin 2\varphi}\dfrac{\partial(u'\phi')}{\partial\lambda} \\ \dfrac{2\Omega\sin\varphi}{S}\left[v'T' - \dfrac{1}{2\Omega a \sin 2\varphi}\dfrac{\partial(T'\phi')}{\partial\lambda}\right] \end{pmatrix} \tag{7}$$

where S is the parameter of static stability, u' is the zonal wind perturbation (deviation from the zonally averaged value), v' is the meridional wind perturbation, T' is the temperature perturbation, ϕ' is the perturbation of the geopotential, Ω is the angular velocity of Earth rotation, λ is the longitude, φ is the latitude, a is the radius of the Earth, p is the pressure, $p_0 = 1000$ hPa.

Fig. 10 shows the evolution of the wave activity flux over the Northern Hemisphere before, during, and after the SSW event. The distribution of the vertical component of wave activity flux at 20 km at about one week after the first SPW1 enhancement in the stratosphere and/or 15 days before the SSW event is shown in Fig. 10a. It is evident that a relatively strong downward flux of wave activity from the stratosphere into the troposphere exists over the Atlantic. To be sure that this flux is capable of reaching the tropospheric heights, meridional sections of the wave activity flux and its divergence averaged over longitudinal sector 80–110 W (over Atlantic) in altitude range 0–20 km have been calculated. The results obtained are presented in Fig. 11. The figure demonstrates that there is a substantial downward flux of wave activity into the troposphere before SSW. The downward wave activity flux in this longitudinal sector can explain the strongest influence of polar vortex events on the tropospheric circulation over North Atlantic (Dunn-Sigouin and Shaw, 2015). This flux

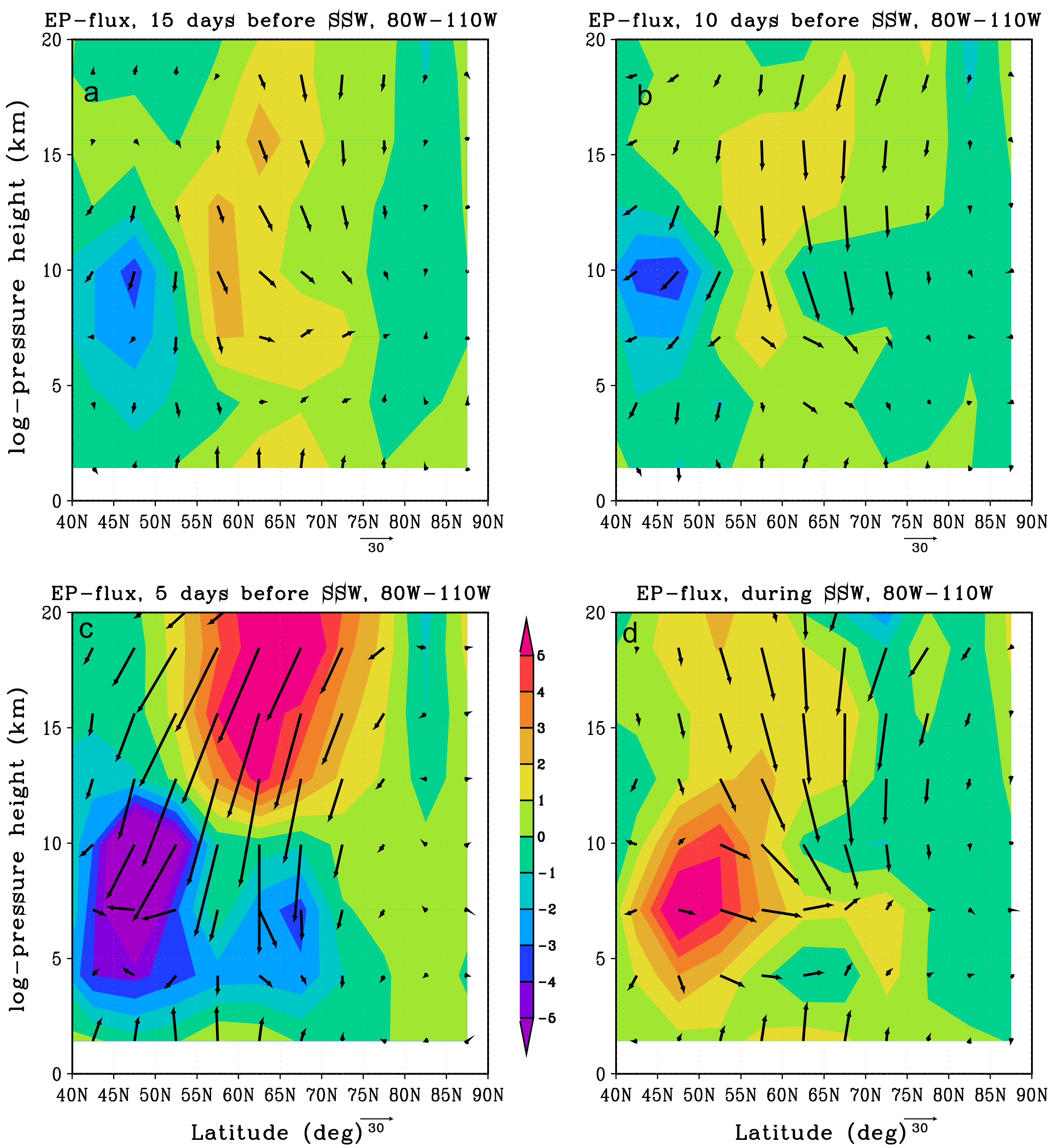

Fig. 11. Latitude–height cross sections of the wave activity flux (arrows) superimposed on its divergence (shaded) averaged over longitudinal sector 80–110 W (Arctic). The vertical components of the flux are shown with factor 100 to make them visible. The units are m^2/s^2 for wave activity flux and m/s/day for the divergence. The distributions are shown at 15, 10, and 5 days before the SSW event (a, b, and c, respectively) and during SSW (d).

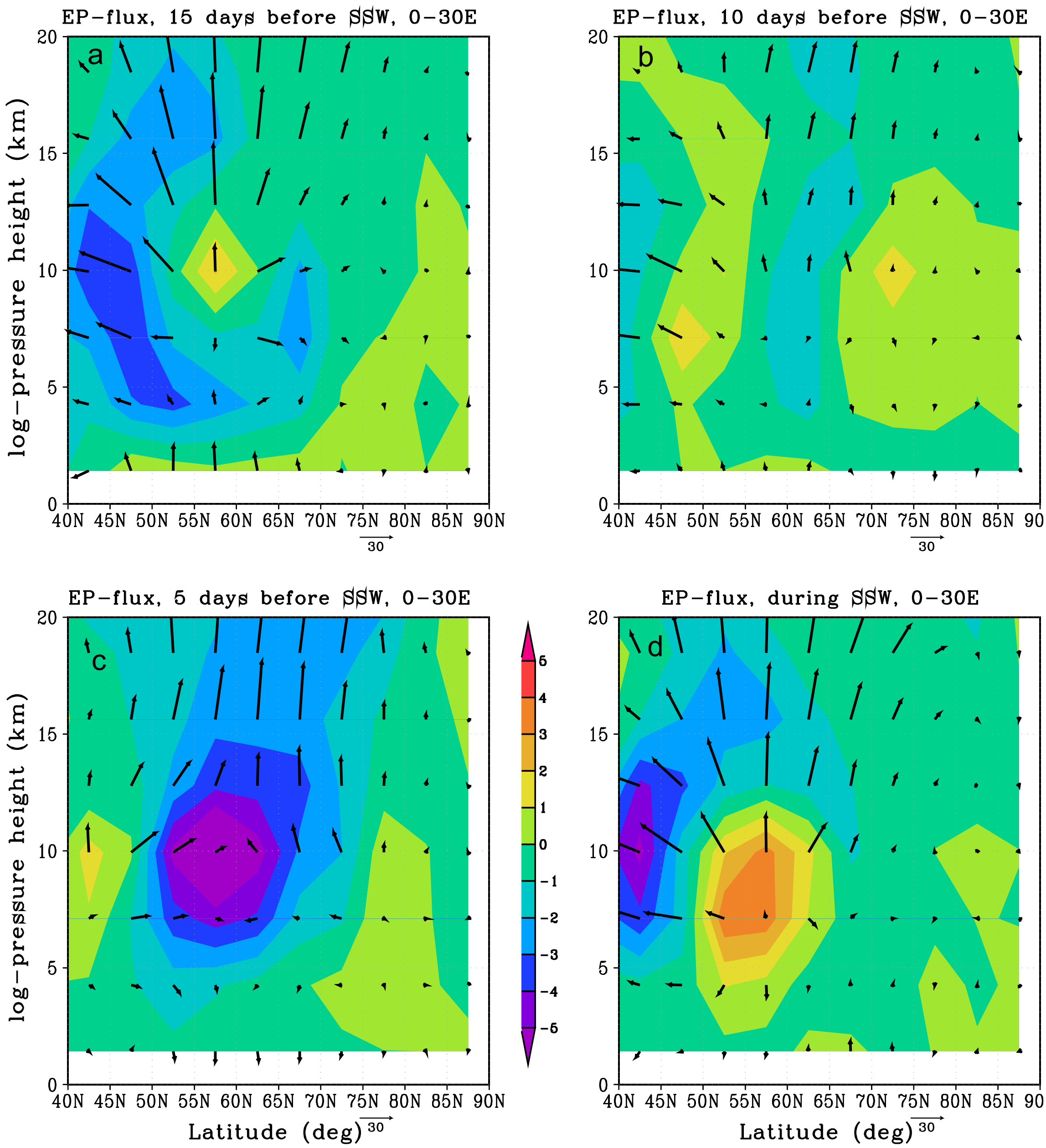

Fig. 12. Latitude–height cross sections of the wave activity flux (arrows) superimposed on its divergence (shaded) averaged over longitudinal sector 0–30E (Europe). The vertical components of the flux are shown with factor 100 to make them visible. The units are m^2/s^2 for wave activity flux and m/s/day for the divergence. The distributions are shown at 15, 10, and 5 days before the SSW event (a, b, and c, respectively) and during SSW (d).

reaches the troposphere and then redistributes within the horizontal plane (Fig. 10b). With the delay of about 5 days, the horizontal flux is directed from the area of maximum wave activity downstream to Europe, where its convergence is seen. Thus, at this time we can expect significant changes in the weather conditions over Europe, including the European part of Russia. Meridional sections of the wave activity flux and its divergence averaged over longitudinal sector 0–30E (over Europe) in altitude range 0–20 km are presented in Fig. 12. This figure shows that during SSW in this region we observe the divergence of wave activity flux in the troposphere and an increase of this flux from the troposphere into the stratosphere.

The vertical component of wave activity flux at 20 km and the distribution of its horizontal component in the troposphere during the development of the SSW event are presented in Fig. 10c. The figure shows a noticeable enhancement of the wave activity flux from the troposphere into the stratosphere, and weakening of the downward flux from the stratosphere into the troposphere during the SSW event. At the same time, horizontal components of the wave activity flux from the downstream area in the direction of Europe are amplified. Our results indicate that about 2–3 weeks before the SSW we observe an enhancement of wave activity flux from the stratosphere into the troposphere. Thus, the primary reason of the wave activity enhancement at the stratospheric altitudes is the nonlinear interaction between the SPW1 and mean flow during the vacillation cycle. The following scenario for the SSW development (at least in terms of the statistical mean, the average over the 15 events) can be inferred from our simulations.

(1) The enhancement of the SPW1 in the upper stratosphere occurs because of an amplification of nonlinear interactions between the SPW1 and mean flow. This enhancement is

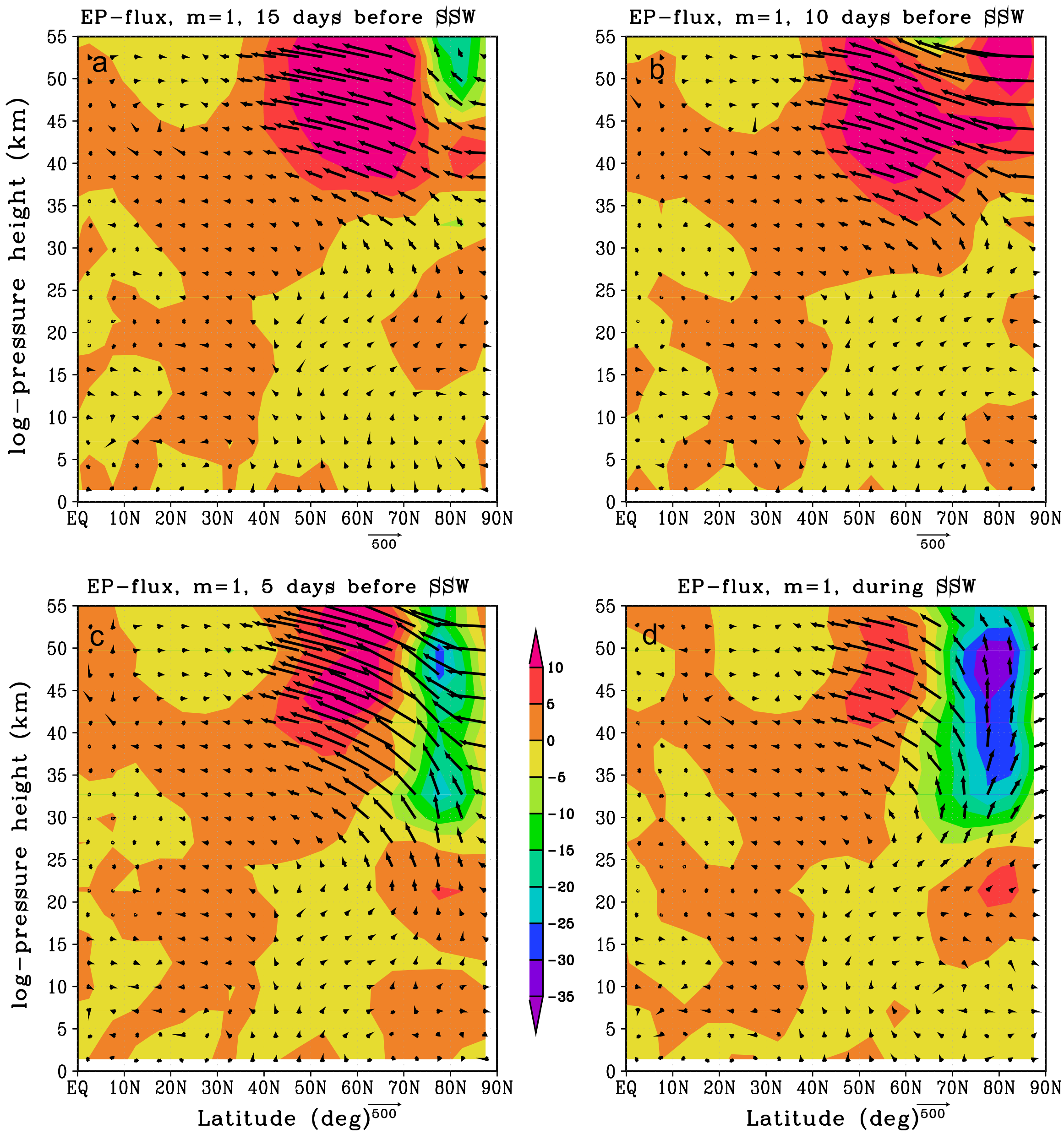

Fig. 13. Latitude–height cross sections of the EP flux vectors (arrows) superimposed on the EP flux divergence (shaded) for SPW1. Both components of the EP flux and its divergence are divided by $\rho_0 a \cos\varphi$. The vertical components of the EP flux are shown with factor 100 to make them visible. The units are m^2/s^2 for EP flux and m/s/day for the EP flux divergence. The distributions are shown at 15, 10, and 5 days before the SSW event (a, b, and c, respectively) and during SSW (d).

accompanied by a subsequent increase of the wave activity flux from the stratosphere into the troposphere.

(2) Further, the wave activity is transported horizontally, and then an increase of the upward flux from the troposphere into the stratosphere in another region takes place (weather anomalies in the troposphere, mainly over Europe, may develop).

(3) The secondary enhancement of the planetary wave activity in the stratosphere is accompanied by a temperature rise in the polar region, and by a weakening or even reversal of the stratospheric jet.

Researchers often focus only on an enhancement of the wave activity flux from the troposphere into the stratosphere, and do not consider the reasons of this enhancement (Cohen and Jones, 2011; Bancala et al., 2012). Our results emphasize the importance of nonlinear processes in the stratosphere that take place before the enhancement of wave activity flux from the troposphere. It is also interesting to consider what happens after the SSW event. Fig. 13e shows the vertical component of wave activity flux at 20 km, and the distribution of the horizontal component of wave activity in the troposphere about 10 days after the onset of the SSW. It is seen that there is a noticeable net enhancement of the wave activity flux from the stratosphere into the troposphere. Although its maximum is approximately same as during the SSW, additional downstream areas appear over North America and Ural mountain range. Redistribution of wave activity in the horizontal plane in the troposphere can lead to its strengthening in the areas located to the east of the region under consideration. As the result, an abnormal weather can be observed not only in Europe, but in Siberia as well. This situation can last for several days. The distribution of the horizontal flux in the troposphere about two weeks after the SSW is shown in Fig. 10f. It is evident that the meteorological processes in the troposphere calm down with time, and the significant weakening of the vertical component of wave activity flux occurs.

7. EP flux diagnostics of SPW propagation

To consider planetary wave propagation and acceleration of the mean flow several days before and during SSW, the Eliassen–Palm (EP) flux (Andrews, 1987) for wave1 and wave2 has been calculated. Latitude–height cross sections of the EP flux vectors (arrows) superimposed on the EP flux divergence (shaded) for SPW1 and SPW2 are presented in Figs. 13 and 14, respectively. The figures show that just before the SSW event EP flux of SPW1 is refracted to the high latitudes in the stratosphere and finally produces a substantial deceleration of the mean flow at higher-middle latitudes in the upper stratosphere. The EP flux for SPW2 is weaker and behavior is different (Fig. 14). In the upper stratosphere we observe a strong positive divergence at middle latitude and EP flux is directed from this region to the polar region and downward producing the deceleration of the mean flow in the higher-middle latitude in the lower stratosphere (Fig. 14d). This result indicates that during SSW in the middle latitude upper stratosphere we have the source of SPW2, which can be caused by nonlinear interactions of this wave with other waves and/or with the mean flow.

8. Conclusions

Based on the results presented above, the following conclusions can be made:

- Analyzing the zonal mean flow and temperature, particularly the standard deviation of the interannual variability of these fields that were averaged over 1992–2011 years, it is possible to make a reasonable guess that QBO phase has to be defined considering the deviation of zonal mean flow from the climatic values at the altitude of about 30 km.

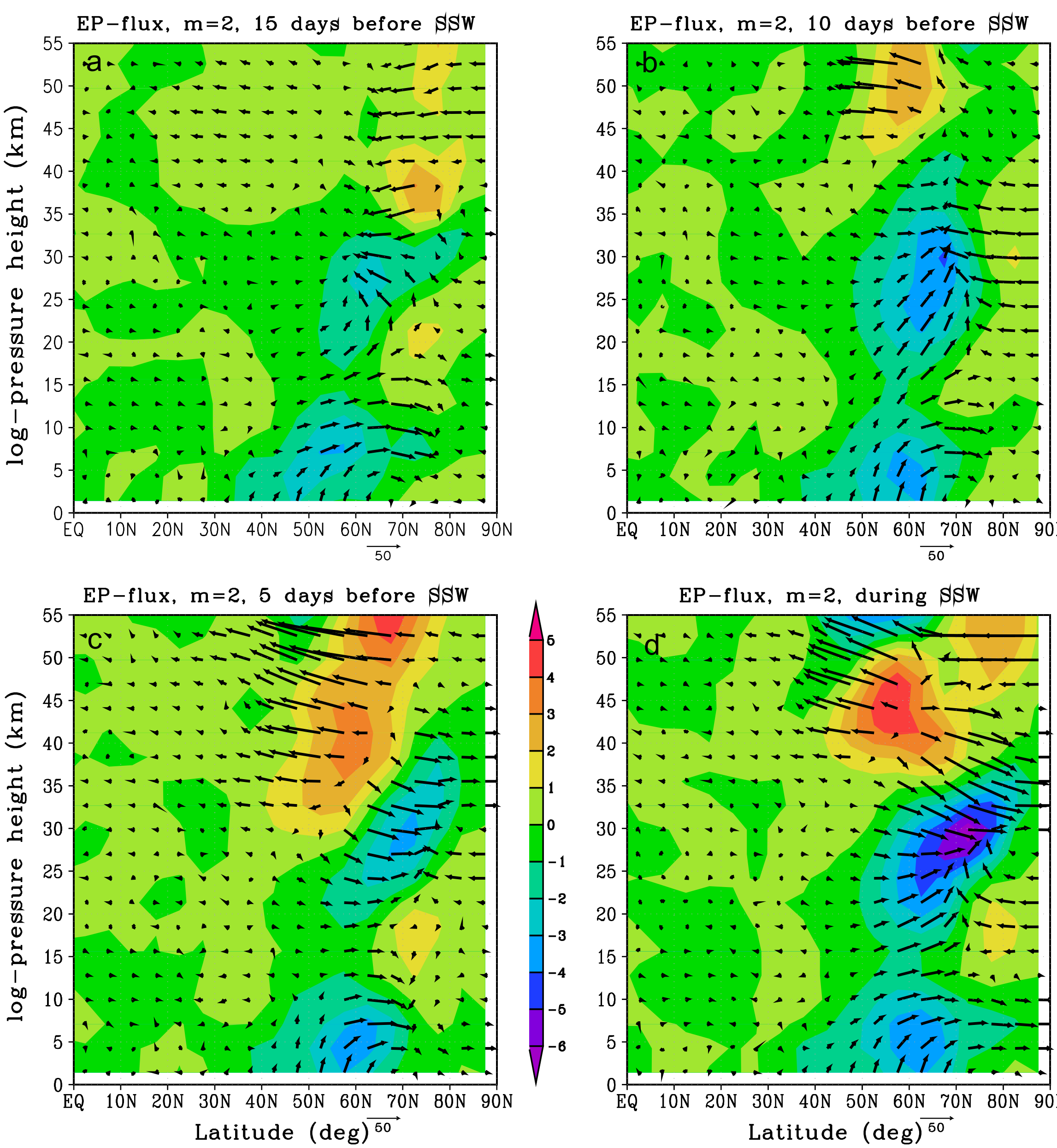

Fig. 14. Latitude–height cross sections of the EP flux vectors (arrows) superimposed on the EP flux divergence (shaded) for SPW2. Both components of the EP flux and its divergence are divided by $\rho_0 a \cos\varphi$. The vertical components of the EP flux are shown with factor 100 to make them visible. The units are m^2/s^2 for EP flux and m/s/day for the EP flux divergence. The distributions are shown at 15, 10, and 5 days before the SSW event (a, b, and c, respectively) and during SSW (d).

- Comparison of the zonal wind and temperature under westerly and easterly QBO phases provides the insight into SSW behavior. The SSW events are more intensive and/or the frequency of these events is higher under the easterly QBO phase.
- To understand the processes responsible for the SSW initiation and development, it is important to consider the dynamical processes in the stratosphere long before – at least 2–3 weeks before the onset of SSWs, or even longer.
- Stratospheric nonlinear processes play an important role in providing a favorable conditions for the SSW initiation, or likely initiate the event themselves.
- The meridional refraction of planetary waves to the polar region is one of the preconditions of development SSW events (McIntyre, 1982). Nevertheless, the nonlinear wave–wave and wave–mean flow interactions can play an important role before and during SSW. These processes can lead to the excitation of SPW in the upper stratosphere.
- The SSW definition recommended by the WMO (Butler et al., 2015) can be reconsidered, at least in respect to the altitude (for instance, these events have to be looked at about 40 km and judged by temperature changes, and/or even higher for the zonal jet reversals).

Acknowledgments

This research was supported by the Russian Science Foundation under Grant 14-17-00685 and by the RFBR under Grant 13-05-91154 in the part of stratosphere–troposphere coupling. Savenkova E.N. acknowledges Saint-Petersburg State University support (Grant 11.50.1048.2014). We are grateful to the UK Met Office and BADC for access to the data.

References

Albers, J.R., Birner, T., 2014. Vortex preconditioning due to planetary and gravity waves prior to sudden stratospheric warmings. J. Atmos. Sci. 71, 4028–4054. http://dx.doi.org/10.1175/JAS-D-14-0026.1.
Andrews, D.G., 1987. On the interpretation of the Eliassen–Palm flux divergence. Q. J. R. Meteorol. Soc. 113, 323–338.
Ayarzaguena, B., Langematz, U., Serrano, E., 2011. Tropospheric forcing of the stratosphere: a comparative study of the two different major stratospheric warmings in 2009 and 2010. J. Geophys. Res. 116, D18114. http://dx.doi.org/10.1029/2010JD015023.
Baldwin, M.P., et al., 2001. The quasi-biennial oscillation. Rev. Geophys. 39, 179–229.
Baldwin, M.P., Dunkerton, T.J., 2001. Stratospheric harbingers of anomalous weather regimes. Science 294, 581–584.
Baldwin, M.P., Dameris, M., Shepherd, T.G., 2007. How will the stratosphere affect climate change? Science 316, 1576–1577.
Bancala, S., Kruger, K., Giorgetta, M., 2012. The preconditioning of major sudden stratospheric warmings. J. Geophys. Res. 117, D04101. http://dx.doi.org/10.1029/2011JD016769.
Butler, A., Seidel, D., Hardiman, S., Butchart, N., Birner, T., Match, A., 2015. Defining sudden stratospheric warmings. Bull. Am. Meteor. Soc., in press. http://dx.doi.org/10.1175/BAMS-D-13-00173.1.
Charlton, A., Polvani, L., 2007. A new look at stratospheric sudden warmings. Part I: climatology and modeling benchmarks. J. Clim. 20, 449–469.
Cohen, J., Jones, J., 2011. Tropospheric precursors and stratospheric warmings. J. Clim. 24. http://dx.doi.org/10.1175/2011JCLI4160.1.
Dunn-Sigouin, E., Shaw, T.A., 2015. Comparing and contrasting extreme stratospheric events, including their coupling to the tropospheric circulation. J. Geophys. Res. Atmos. 120, 1374–1390. http://dx.doi.org/10.1002/2014JD022116.
Esler, J.G., Polvani, L.M., Scott, R.K., 2006. The Antarctic stratospheric sudden warming of 2002: a self-tuned resonance?. Geophys. Res. Lett. 33, L12804. http://dx.doi.org/10.1029/2006GL026034.
Fuller-Rowell, T., Wu, F., Akmaev, R., Fang, T.-W., Araujo-Pradere, E., 2010. A whole atmosphere model simulation of the impact of a sudden stratospheric warming on thermosphere dynamics and electrodynamics. J. Geophys. Res. 115, A00G08. http://dx.doi.org/10.1029/2010JA015524.
Funke, B., Lopez-Puertas, M., Bermejo-Pantaleon, D., Garcia-Comas, M., Stiller, G.P., von Clarmann, T., Kiefer, M., Linden, A., 2010. Evidence for dynamical coupling from the lower atmosphere to the thermosphere during a major stratospheric warming. Geophys. Res. Lett. 37, L13803. http://dx.doi.org/10.1029/2010GL043619.
Holton, J.R., 1980. The dynamics of sudden stratospheric warmings. Ann. Rev. Earth Planet. Sci. 8, 169–190.
Holton, J.R., Mass, C., 1976. Stratospheric vacillation cycles. J. Atmos. Sci. 33, 2218–2225.
Holton, J.R., Tan, H.-C., 1980. The influence of the equatorial quasi-biennial oscillation on the global circulation at 50 mb. J. Atmos. Sci. 37, 2200–2208.
Inoue, M., Takahashi, M., Naoe, H., 2011. Relationship between the stratospheric quasi-biennial oscillation and tropospheric circulation in northern autumn. J. Geophys. Res. 116, D24115. http://dx.doi.org/10.1029/2011JD016040.
Kurihara, J., Ogawa, Y., Oyama, S., Nozawa, S., Tsutsumi, M., Hall, C.M., Tomikawa, Y., Fujii, R., 2010. Links between a stratospheric sudden warming and thermal structures and dynamics in the high-latitude mesosphere, lower thermosphere, and ionosphere. Geophys. Res. Lett. 37, L13806. http://dx.doi.org/10.1029/2010GL043643.
Kuttippurath, J., Nikulin, G., 2012. The sudden stratospheric warming of the Arctic winter 2009/2010: comparison to other recent warm winters. Atmos. Chem. Phys. Discuss. 12, 7243–7271.
Labitzke, K., 1977. Interannual variability of the winter stratosphere in the Northern winter. Mon. Weather Rev. 105, 762–770.
Labitzke, K., Naujokat, B., 2000. The lower Arctic stratosphere in winter since 1952. SPARC Newslett. 15, 11–14.
Labitzke, K., Naujokat, B., Kunze, M., 2005. The lower Arctic stratosphere in winter since 1952: an update. SPARC Newslett. 24, 27–28.
Labitzke, K., Kunze, M., 2009. On the remarkable Arctic winter in 2008/2009. J. Geophys. Res. 114, D00102. http://dx.doi.org/10.1029/2009JD012273.
Liu, H., Doornbos, E., Yamamoto, M., Ram, S.T., 2011. Strong thermospheric cooling during the 2009 major stratosphere warming. Geophys. Res. Lett. 38, L12102. http://dx.doi.org/10.1029/2011GL047898.
Matsuno, T., 1971. A dynamical model of sudden stratospheric warming. J. Atmos. Sci. 28, 871–883.
McIntyre, M.E., 1982. How well do we understand the dynamics of stratospheric warmings. J. Meterol. Soc. Jpn. 60, 37–64.
Naoe, H., Shibata, K., 2010. Equatorial quasi-biennial oscillation influence on northern winter extratropical circulation. J. Geophys. Res. 115, D19102. http://dx.doi.org/10.1029/2009JD012952.
Pancheva, D., Mukhtarov, P., 2011. Stratospheric warmings: the atmosphere–ionosphere coupling paradigm. J. Atmos. Sol.-Terr. Phys. 73, 1697–1702. http://dx.doi.org/10.1016/j.jastp.2011.03.006.
Pedatella, N.M., Forbes, J.M., 2010. Evidence for stratosphere sudden warming—ionosphere coupling due to vertically propagating tides. Geophys. Res. Lett. 37, L11104. http://dx.doi.org/10.1029/2010GL043560.
Plumb, R.A., 1985. On the three-dimensional propagation of stationary waves. J. Atmos. Sci. 42, 217–229.
Pogoreltsev, A.I., 2007. Generation of normal atmospheric modes by stratospheric vacillations. Izv. Atmos. Ocean. Phys. 43, 423–435.
Pogoreltsev, A.I., Kanukhina, A.Yu., Suvorova, E.V., Savenkova, E.N., 2009. Variability of planetary waves as a signature of possible climatic changes. J. Atmos. Sol.-Terr. Phys. 71, 1529–1539.
Pogoreltsev, A.I., Savenkova, E.N., Pertsev, N.N., 2014. Sudden stratospheric warmings: the role of normal atmospheric modes. Geomagn. Aeron. 54, 357–372.
Scaife, A.A., Austin, J., Butchart, N., Pawson, S., Keil, M., James, I.N., 2000. Seasonal and interannual variability of the stratosphere diagnosed from UKMO TOVS analyses. Q. J. R. Meterol. Soc. 126, 2585–2604.
Scott, R.K., Polvani, L.M., 2006. Internal variability of the winter stratosphere. Part I: time independent forcing. J. Atmos. Sci. 63, 2758–2776.
Siskind, D.E., Eckermann, S.D., McCormack, J.P., Coy, L., Hoppel, K.W., Baker, N.L., 2010. Case studies of the mesospheric response to recent minor, major and extended stratospheric warmings. J. Geophys. Res. 115, D00N03. http://dx.doi.org/10.1029/2010JD014114.
Smith, A.K., 1983. Observation of wave–wave interaction in the stratosphere. J. Atmos. Sci. 40, 2484–2496.
Smith, A.K., Gille, J.C., Lyjak, L.W., 1984. Wave–wave interactions in the stratosphere: observations during quiet and active wintertime period. J. Atmos. Sci. 41, 363–373.
Stan, C., Straus, D.M., 2009. Stratospheric predictability and sudden stratospheric warming events. J. Geophys. Res. 114, D12103. http://dx.doi.org/10.1029/2008JD011277.
Sun, L., Robinson, W.A., 2009. Downward influence of stratospheric final warming events in an idealized model. Geophys. Res. Lett. 36, L03819. http://dx.doi.org/10.1029/2008GL036624.
Sun, L., Robinson, W.A., Chen, G., 2011. The predictability of stratospheric warming events: more from the troposphere or the stratosphere?. J. Atmos. Sci. 69. http://dx.doi.org/10.1175/JAS-D-11-0144.1.
Swinbank, R., O'Neill, A., 1994. A stratosphere–troposphere assimilation system. Mon. Weather Rev. 122, 686–702.
Waugh, D.W., et al., 2010. Persistence of the lower stratospheric polar vortices. J. Geophys. Res. 104, 27191–27202.
Welch, B.L., 1947. The generalization of "Student's" problem when several different population variances are involved. Biometrika 34, 28–35.
Yuan, T., Thurairajah, B., She, C.-Y., Chandran, A., Collins, R.L., Krueger, D.A., 2012. Wind and temperature response of midlatitude mesopause region to the 2009 sudden stratospheric warming. J. Geophys. Res. 117, D09114. http://dx.doi.org/10.1029/2011JD017142.